 CMES, vol.72, no.2, pp.79-102, 2011

Probabilistic Dynamic Analysis of Vehicle-Bridge Interaction System with Uncertain Parameters

N. Liu,[1] W. Gao[1] C.M. Song[1] and N. Zhang [2]

Abstract: This paper presents the probabilistic dynamic analysis of vehicle-bridge interaction systems. The bridge's and vehicle's parameters are considered as random variables as well as the road surface roughness is modeled as random process. A two-degree-of-freedom spring-mass system is used to represent a moving vehicle and the bridge is modeled as an Euler-Bernoulli beam. From the equation of motion for the vehicle-bridge coupling system, the expressions for mean value and standard deviation of bridge response are developed by using the random variable's functional moment method. The effects of the individual system parameters and the road surface roughness on the bridge response are investigated. Monte-Carlo simulation method is used to verify the approach presented in this paper. The effectiveness of the proposed method is also demonstrated by numerical examples.

Keywords: Vehicle-bridge interaction system, probabilistic dynamic analysis, random parameters, road surface roughness, numerical characteristics.

1 Introduction

The dynamic response analysis of vehicle-bridge system is one of the most crucial steps in bridge design as moving vehicles induced vibrations make significant contribution to the fatigue of bridges. Over the past few decades, the interactive problem between vehicles and bridge structures has attracted much more attention due to the rapid increase in the proportion of vehicles and high-speed vehicles in highway and railway traffic [Dey and Balasubramanian (1984); Rassem, Ghobarah, and Heidebrecht (1996); Yang and Wu (2001); Kwasniewski, Li, Wekezer, and Malachowski (2006); Yin, Fang, Cai, and Deng (2010)]. Fryba [Fryba (1999)] presented the analytical solutions for simply supported and continuous beams with

[1] School of Civil and Environmental Engineering, The University of New South Wales, Sydney, NSW 2052, Australia

[2] School of Electrical, Mechanical and Mechatronic Systems, University of Technology, Sydney, NSW 2007, Australia

uniform cross-section under moving loads. Green and Cebon [Green and Cebon (1994)] gave the solution on the dynamic response of an Euler-Bernoulli beam under a "quarter-car" vehicle model in the frequency domain using an iterative procedure with experimental verification. Yang and Lin [Yang and Lin (2005)] investigated the dynamic interaction between a moving vehicle and the supporting bridge by means of the modal superposition technique with closed-form solution. The beam bridge model was extended by Law and Zhu [Law and Zhu (2005)] to an orthotropic rectangular plate simply supported on a pair of parallel edges under a stream of moving loads based on the Lagrange equation and modal superposition. Yang and Chang[Yang and Chang (2009a,b)] studied the extraction of the bridge frequencies from the dynamic response of a passing vehicle using the beam and moving spring-mass model.

In the conventional dynamic analysis of a vehicle-bridge interaction system, the vehicle's and bridge's parameters are treated as deterministic [Sridharan and Mallik (1979); Wu and Dai (1987); Muscolino, Ricciardi, and Impollonia (2000); Yang and Chang (2009a,b)]. The conventional deterministic analysis represents only an "approximation" of the results due to uncertainties in the structural properties as well as in the loading processes. Generally speaking, vehicles moving on a bridge have nondeterministic characteristics because the parameters of different types of vehicles are different. Parameters of a bridge, i.e. mass, Young's modulus, and moment of inertial and so on, are usually having uncertainty resulting from construction and manufacturing tolerances or caused by corrosion of steel and deterioration of concrete during its lifetime. The road pavement roughness also has significantly random characteristics in vehicle-bridge interaction system. Some research have been carried out on the dynamic response of a bridge deck with the road surface roughness. Gupta [Gupta, Hughes, and Sellars (1980)] used a sine function to simulate the road surface roughness. In order to take into account its random characteristic, a stationary Gaussian random process with certain power spectral density function is used to describe the road roughness profile [Hwang and Nowak (1991); Kim, Kawatani, and Kim (2005); Law and Zhu (2005); Ding, Hao, and Zhu (2009)]. Recently, some pioneering research on stochastic dynamic analysis of vehicle-bridge interaction systems have been conducted considering uncertainties in bridge parameters or in moving loadings [Ding, Hao, and Zhu (2009); Wu and Law (2010a)]. The uncertainty of the moving loadings are caused by the road surface roughness or vehicle's speed. However, for real engineering applications and the quantitative dynamic analysis response of bridges, the uncertainty of vehicle's parameters should be also included in the analytical model. In addition, it is very important to investigate the effect of an individual system parameter on the bridge's response.

The most common approach to problems of uncertainty is to model the system parameters as random variables. Over the past twenty years, probabilistic methods such as Monte-Carlo simulation method (MCSM) [Marek, Brozzetti, Gustar, and Elishakoff (2002); Radhika, Panda, and Manohar (2008)], perturbation method (PM) [Xia, Hao, Brownjohn, and Xia (2002)], stochastic finite element method [Baroth, Bressolette, Chauvière, and Fogli (2007); Manjuprasad and Manohar (2007)] and spectral stochastic finite element method (SSFEM) [Ghanem and Spanos (2003); Gaignaire, Clénet, Sudret, and Moreau (2007); Wu and Law (2010b)] have been widely used in the static and dynamic analysis of structures with random parameters. To reduce the computational effort and simultaneously investigate the effect of the individual system parameters on the structural responses, the random variable's functional moment Method (RVFMM) has also been developed to analyze structures with uncertain parameters [Gao (2007); Gao, Zhang, and Dai (2008); Gao, Song, and Tin-Loi (2009, 2010)].

In this paper, the random variable's functional moment method is employed to study the dynamic response of vehicle-bridge interaction system by considering the effect of the road surface roughness and the uncertainties in bridge's and vehicle's parameters. The moving vehicle is represented by a two-degree-of-freedom vehicle model and the bridge is treated as an Euler-Bernoulli beam. The expressions for the mean value and standard deviation of bridge response are developed. The effects produced by the road surface roughness, bridge's and vehicle' parameters on bridge response are also investigated.

2 Formulation of the vehicle and the bridge model

2.1 Road surface roughness

In this study, the road surface roughness is regarded as a periodic modulated random process. In ISO-8608(20) specifications, the road roughness is related to the vehicle velocity by a formula between the velocity power spectral density (PSD) and the displacement PSD. The common formulation of displacement PSD of the roughness is [Honda, Kajikawa, and Kobori (1982); Au, Cheng, and Cheung (2001)]:

$$S_r(w_s) = A_r \cdot (\frac{w_s}{w_{so}})^{-a} \tag{1}$$

where $S_r(w_s)$ is the displacement PSD of the road surface roughness, A_r is the roughness coefficient in m^2 /cycle/m, w_{so} is the reference spatial frequency, a is an exponent of the PSD and w_s is the spatial frequency in cycle/m,respectively. In the time domain, the road surface roughness function $r(x)$ is given by:

$$r(x) = \sum_{k=1}^{N} ([4A_r(\frac{(2\pi k)}{L_c w_{so}})^{-2}]^{1/2} \cdot \cos(w_{sk}x - \varphi_k)) \tag{2}$$

where

$$w_{sk} = k \cdot \Delta w_s, k = 1,2,\cdots N, \Delta w_s = 2\pi / L_c \tag{3}$$

$$w_{so} = \frac{1}{2\pi} \tag{4}$$

L_c is twice the length of the bridge, φ_k is generated between 0 and 2π by using the Monte Carlo simulation.

2.2 Bridge and vehicle models

In the vehicle-bridge interaction system demonstrated in Fig. 1, the bridge is modeled as an Euler-Bernoulli beam and the vehicle is represented by a quarter-car model. Over the years various types of bridge models have been used in studies on bride-vehicle dynamics. Continuum models of simply-supported Euler-Bernoulli beams are the most popular ones, mainly due to its simplicity and ability to obtain closed-form solution. The two-degree-of-freedom quarter-car model is generally reputed to be sufficiently accurate for capturing the essential features of dynamic performance of a moving vehicle [Gao, Zhang, and Dai (2008)].

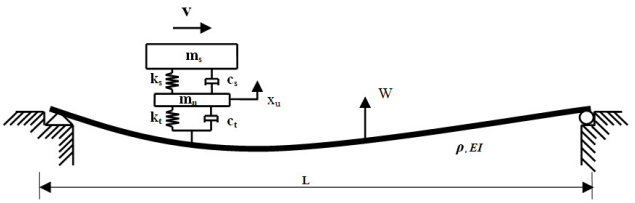

Figure 1: Model of a coupled vehicle-bridge system.

The equation of motion for the bridge can be expressed as follows:

$$\rho A \frac{\partial^2 W(x,t)}{\partial t^2} + C \frac{\partial W(x,t)}{\partial t} + EI \frac{\partial^4 W(x,t)}{\partial x^4} = f(x,t)\delta(x - vt), \tag{5}$$

where ρ is the mass density, A is the cross-sectional area, C is viscous proportional damping, E is the elastic modulus (Young's modulus) and I is the moment of inertia, respectively. $W(x,t)$ is the displacement function which varies with the time

t and the location x. $f(x,t)$ is the interactive force, v is the velocity of the vehicle and $\delta(x-vt)$ is the Dirac delta function evaluated at the contact point $x=vt$.

For a smooth road surface, $f(x,t)$ can be expressed as:

$$f(x,t) = k_t[x_u - w] + C_t[\dot{x}_u - \dot{w}] - (m_u + m_s)g \tag{6}$$

where k_t, C_t, m_u and m_s are the tire stiffness, tire damping, unsprung mass and sprung mass of the vehicle, respectively.

Considering the roughness of the road surface, $f(x,t)$ is rewritten as:

$$f(x,t) = k_t[x_u - w - r(x)] + C_t[\dot{x}_u - \dot{w} - \dot{r}(x)] - (m_u + m_s)g \tag{7}$$

where $r(x)$ is the road surface roughness of the bridge.

Using the model superposition method, the bridge response can be calculated with the following equation:

$$W(x,t) = \sum_{j=1}^{\infty} \sin\frac{j\pi x}{L} x_{bj}(t) \tag{8}$$

where $x_{bj}(t)$ is the jth modal displacement and L is the length of the bridge.

3 Analysis of the dynamic response of vehicle-bridge interaction system

3.1 Dynamic response analysis of bridge with smooth road surface

Substituting Eqs. (6) and (8) into Eq. (5) yields:

$$\begin{aligned}
&\int_0^L \rho\phi_j^T(x) \sum_{j=1}^{\infty} \phi_j(x)\ddot{x}_{bj}(t)dx + \int_0^L C\phi_j^T(x) \sum_{j=1}^{\infty} \phi(x)\dot{x}_{bj}(t)dx \\
&+ \int_0^L EI\phi_j^T(x) \cdot \sum_{j=1}^{\infty} \frac{\partial^4\phi_j(x)}{\partial x^4} x_{bj}(t)dx \\
&= \int_0^L \rho\phi_j^T(x)[K_t[x_u - W|_{x=vt}] + C_t[\dot{x}_u - \dot{W}|_{x=vt} - (m_s+m_u)g]\delta(x-vt)dx
\end{aligned} \tag{9}$$

where $\phi_j(x) = \sin\frac{j\pi x}{L}$.

Eq. (9)can be rewritten as:

$$\begin{aligned}
\rho\ddot{x}_{bj}(t)\cdot\frac{L}{2} + C\dot{x}_{bj}(t)\cdot\frac{L}{2} + EI\cdot(\frac{j\pi}{L})^4\cdot\frac{L}{2}\cdot x_{bj}(t) = &-(m_s+m_u)g\cdot\sin\frac{j\pi vt}{L} \\
&+K_t(x_u - W|_{x=vt})\cdot\sin\frac{j\pi vt}{L} + C_t(\dot{x}_u - \dot{W}|_{x=vt})\cdot\sin\frac{j\pi vt}{L}
\end{aligned} \tag{10}$$

Dividing the two sides of Eq. (10) by $\rho \cdot \frac{L}{2}$, we have:

$$\begin{aligned}\ddot{x}_{bj}(t)+\frac{C}{\rho}\dot{x}_{bj}(t)+\frac{EI}{\rho}\cdot(\frac{j\pi}{L})^4\cdot x_{bj}(t) = &-\frac{2(m_s+m_u)g}{\rho L}\cdot\sin\frac{j\pi vt}{L}\\ &+\frac{2K_t(x_u-W|_{x=vt})}{\rho L}\cdot\sin\frac{j\pi vt}{L}\\ &+\frac{2C_t(\dot{x}_u-\dot{W}|_{x=vt})}{\rho L}\cdot\sin\frac{j\pi vt}{L}\end{aligned} \tag{11}$$

Assuming that the vehicle mass is much less than the bridge mass [Yang and Lin (2005)], Eq. (16) can be approximated as:

$$\ddot{x}_{bj}(t)+2\zeta_{bj}\omega_{bj}\cdot\dot{x}_{bj}(t)+\omega_{bj}^2\cdot\dot{x}_{bj}(t) = -\frac{2(m_s+m_u)g}{\rho L}\cdot\sin\frac{j\pi vt}{L} \tag{12}$$

where $\omega_{bj}=\frac{j^2\pi^2}{L^2}\cdot\sqrt{\frac{EI}{\rho}}$, and $\zeta_{bj}=\frac{C}{2\rho\omega_{bj}}$ is the jth modal damping ratio of the bridge.

The solution of Eq. (12) can be obtained by using the Convolution Integral (Duhamel Integral):

$$x_{bj}=\frac{1}{\omega_{bj}}\int_0^t e^{-\zeta_{bj}\omega_{bj}(t-\tau)}\sin\omega_{dbj}(t-\tau)\cdot(-\frac{2(m_s+m_u)g}{\rho L}\cdot\sin\frac{j\pi v\tau}{L})d\tau \tag{13}$$

Eq. (13) can be rewritten as:

$$x_{bj}=-\frac{2(m_s+m_u)g}{\rho L\omega_{dbj}}\int_0^t e^{-\zeta_{bj}\omega_{bj}(t-\tau)}\sin\omega_{dbj}(t-\tau)\cdot\sin\frac{j\pi v\tau}{L}d\tau \tag{14}$$

From Eq. (8) and Eq. (14), the bridge response can be calculated by:

$$W(x,t)=-\frac{2(m_s+m_u)g}{\rho L\omega_{dbj}}\sum_{j=1}^{\infty}\sin\frac{n\pi x}{L}\int_0^t e^{-\zeta_{bj}\omega_{bj}(t-\tau)}\sin\omega_{dbj}(t-\tau)\cdot\sin\frac{j\pi v\tau}{L}d\tau \tag{15}$$

where $\omega_{dbj}=\sqrt{1-\zeta_{bj}^2}\omega_{bj}$

3.2 Dynamic response of bridge considering road surface roughness

Similarly, substituting Eqs. (7) and (8) into Eq. (5) yields

$$\begin{aligned}&\int_0^L \rho\phi_j^T(x)\sum_{j=1}^{\infty}\phi(x)\ddot{x}_{bj}(t)dx+\int_0^L C\phi_j^T(x)\sum_{j=1}^{\infty}\phi(x)\dot{x}_{bj}(t)dx\\&\qquad+\int_0^L EI\phi_j^T(x)\cdot\sum_{j=1}^{\infty}\frac{\partial^4\phi_j(x)}{\partial x^4}x_{bj}(t)dx\\&=\int_0^L \rho\phi_j^T(x)[k_t[x_u-W|_{x=vt}-r(x)]\\&\qquad+C_t[\dot{x}_u-\dot{W}|_{x=vt}-\dot{r}(x)-(m_s+m_u)g]\delta(x-vt)dx\end{aligned}\tag{16}$$

Eq. (16) can be rewritten as :

$$\begin{aligned}&\rho\ddot{x}_{bj}(t)\int_0^L\sin^2\frac{j\pi x}{L}dx+C\dot{x}_{bj}(t)\int_0^L\sin^2\frac{j\pi x}{L}dx+EI(\frac{n\pi}{L})^4x_{bj}(t)\int_0^L\sin^2\frac{j\pi x}{L}dx\\&=-(m_s+m_u)g\int_0^L\sin\frac{j\pi x}{L}\delta(x-vt)dx+k_t(x_u-W|_{x=vt})\int_0^L\sin\frac{j\pi x}{L}\delta(x-vt)dx\\&\qquad+C_t(\dot{x}_u-\dot{W}|_{x=vt})\int_0^L\sin\frac{j\pi x}{L}\delta(x-vt)dx\\&\qquad-\int_0^L[k_tr(x)+C_t\dot{r}(x)]\sin\frac{j\pi x}{L}\delta(x-vt)dx\end{aligned}\tag{17}$$

Eq. (17) can be further developed as:

$$\begin{aligned}\ddot{x}_{bj}(t)+2\zeta_{bj}\omega_{bj}\cdot\dot{x}_{bj}(t)+\omega_{bj}^2\cdot\dot{x}_{bj}(t)=&-\frac{2(m_s+m_u)g}{\rho L}\cdot\sin\frac{j\pi vt}{L}\\&-\frac{2[k_tr(x)+C_t\dot{r}(x)]}{\rho L}\cdot\sin\frac{j\pi vt}{L}\end{aligned}\tag{18}$$

Then, the jth modal displacement can be obtained as:

$$\begin{aligned}x_{bj}=&-\frac{2}{\rho L\omega_{dbj}}\int_0^t((m_s+m_u)g-[k_tr(x)+C_t\dot{r}(x)])e^{-\zeta_{bj}\omega_{bj}(t-\tau)}\sin\omega_{dbj}(t-\tau)\\&\cdot\sin\frac{j\pi v\tau}{L}d\tau\end{aligned}\tag{19}$$

Therefore, the bridge response can be expressed as:

$$W(x,t) = -\frac{2}{\rho L \omega_{dbj}} \sum_{j=1}^{\infty} \sin\frac{j\pi x}{L} \int_0^t ((m_s+m_u)g - [k_t r(x) + C_t \dot{r}(x)]) \cdot e^{-\zeta_{bj}\omega_{bj}(t-\tau)} \sin\omega_{dbj}(t-\tau) \cdot \sin\frac{j\pi v\tau}{L} d\tau \tag{20}$$

4 Mean value and variance of bridge response

In this study, the vehicle's and bridge's parameters, such as m_s, m_u, ρ, E and I, are considered as random variables. The mean value (u) and standard deviation (σ) of the each random variable are given respectively. The coefficient of variation $v = \sigma/\mu$ is also used to describe the dispersal degree of a random variable. In the following, the expressions for the mean value and variance of bridge displacement response are developed by means of the random variable functional moment method (RVFMM) [Gao, Zhang, and Dai (2008)]. The uncertainty of bridge's parameters will lead to the randomness of its natural frequencies. Consequently, the combination of uncertainties in bridge's dynamic characteristics, system parameters and road surface will result in the randomness of bridge response.

4.1 Numerical characteristics of bridge response with smooth road surface

From Eq. (15) and by using the RVFMM, the mean value of the bridge displacement can be expressed as :

$$\mu_{W(x,t)} = -\frac{2(\mu_{m_s}+\mu_{m_u})g}{S_1\sqrt{\mu_\rho \mu_E \mu_I}} \sum_{j=1}^{\infty} \sin\frac{j\pi x}{\mu_L} \int_0^t S_2 \sin(S_3) \cdot \sin\frac{j\pi v\tau}{\mu_L} d\tau \tag{21}$$

where

$$\mu_I = \frac{1}{12}\mu_b \mu_h^3$$

$$\mu_{\omega_{bj}} = \frac{j^2\pi^2}{\mu_L^2}\sqrt{\frac{\mu_E \mu_h^2}{12\mu_\rho}}$$

$$S_1 = \mu_L\sqrt{1-\zeta_{bj}^2}\frac{j^2\pi^2}{\mu_L^2}$$

$$S_2 = e^{-\mu_{\zeta_{bj}}\mu_{\omega_{bj}}(t-\tau)} \sin\mu_{\omega_{dbj}}(t-\tau)$$

$$S_3 = \sqrt{1-\zeta_{bj}^2}\frac{j^2\pi^2}{\mu_L^2}\sqrt{\frac{\mu_E\mu_I}{\mu_\rho}}(t-\tau)$$

The variance of bridge displacement response can be calculated by:

$$\begin{aligned}\sigma^2_{W(x,t)} = &[\frac{\partial W_{(x,t)}}{\partial m_s}]^2 \cdot \sigma^2_{m_s} + [\frac{\partial W(x,t)}{\partial m_u}]^2 \cdot \sigma^2_{m_u} + [\frac{\partial W_{(x,t)}}{\partial \rho}]^2 \cdot \sigma^2_{\rho} \\ &+ [\frac{\partial W_{(x,t)}}{\partial L}]^2 \cdot \sigma^2_{L} + [\frac{\partial W_{(x,t)}}{\partial I}]^2 \cdot \sigma^2_{I} + [\frac{\partial W_{(x,t)}}{\partial E}]^2 \cdot \sigma^2_{E}\end{aligned} \tag{22}$$

where

$$\frac{\partial W(x,t)}{\partial m_s} = -\frac{2(1+\mu_{m_u})g}{S_1\sqrt{\mu_\rho \mu_E \mu_I}} \sum_{j=1}^{\infty} \sin\frac{j\pi \cdot x}{\mu_L} \int_0^t S_2 \sin(S_3) \sin\frac{j\pi v\tau}{\mu_L} d\tau \tag{23}$$

$$\begin{aligned}\frac{\partial W(x,t)}{\partial m_u} = &-\frac{2(1+\mu_{m_s})g}{\mu_A \mu_\rho \mu_L \mu_{\omega_{dbj}}} \sum_{j=1}^{\infty} \sin\frac{j\pi \cdot x}{\mu_L} \\ &\int_0^t e^{-\mu_{\zeta_{bj}}\mu_{\omega_{bj}}(t-\tau)} \sin\mu_{\omega_{dbj}}(t-\tau) \sin\frac{j\pi v\tau}{\mu_L} d\tau\end{aligned} \tag{24}$$

$$\begin{aligned}\frac{\partial W(x,t)}{\partial E} = &\frac{4(\mu_{m_u}+\mu_{m_s})g}{\mu_A \mu_\rho \mu_L \mu_{\omega_{dbj}}} \sum_{j=1}^{\infty} \sin\frac{j\pi \cdot x}{\mu_L} \\ &\int_0^t e^{-\mu_{\zeta_{bj}}\mu_{\omega_{bj}}(t-\tau)} \sin\mu_{\omega_{dbj}}(t-\tau) \sin\frac{j\pi v\tau}{\mu_L} d\tau\end{aligned} \tag{25}$$

$$\begin{aligned}\frac{\partial W(x,t)}{\partial I} = &\frac{(\mu_{m_u}+\mu_{m_s})g}{S_1\sqrt{\mu_\rho \mu_E \mu_I^3}} \sum_{j=1}^{\infty} \sin\frac{j\pi \cdot x}{\mu_L} \int_0^t S_2 \sin(S_3) \sin\frac{j\pi v\tau}{\mu_L} d\tau \\ &+ \frac{(\mu_{m_u}+\mu_{m_s})g}{S_1\sqrt{\mu_\rho \mu_E \mu_I}} \int_0^t S_2 \zeta_{bj} \frac{j^2\pi^2}{\mu_L^2} \cdot \sqrt{\frac{\mu_E}{\mu_I \mu_\rho}} (t-\tau) \sin(S_3) \sin\frac{j\pi v\tau}{\mu_L} d\tau\end{aligned} \tag{26}$$

$$\begin{aligned}\frac{\partial W(x,t)}{\partial \rho} = &\frac{(\mu_{m_u}+\mu_{m_s})g}{S_1\sqrt{\mu_\rho^3 \mu_E \mu_I}} \sum_{j=1}^{\infty} \sin\frac{j\pi \cdot x}{\mu_L} \int_0^t S_2 \sin(S_3) \sin\frac{j\pi v\tau}{\mu_L} d\tau \\ &+ \frac{(\mu_{m_u}+\mu_{m_s})g}{S_1\sqrt{\mu_\rho \mu_E \mu_I}} \int_0^t S_2 \zeta_{bj} \frac{j^2\pi^2}{\mu_L^2} \cdot \sqrt{\frac{\mu_E \mu_I}{\mu_\rho^3}} (t-\tau) \sin(S_3) \sin\frac{j\pi v\tau}{\mu_L} d\tau\end{aligned} \tag{27}$$

$$\begin{aligned}\frac{\partial W(x,t)}{\partial L} = &\frac{(\mu_{m_u}+\mu_{m_s})g}{S_1\sqrt{\mu_\rho^3 \mu_E \mu_I}} \sum_{j=1}^{\infty} \sin\frac{j\pi \cdot x}{\mu_L} \int_0^t S_2 \sin(S_3) \sin\frac{j\pi v\tau}{\mu_L} d\tau \\ &+ \frac{(\mu_{m_u}+\mu_{m_s})g}{S_1\sqrt{\mu_\rho \mu_E \mu_I}} \int_0^t S_2 \zeta_{bj} \frac{j^2\pi^2}{\mu_L^2} \cdot \sqrt{\frac{\mu_E \mu_I}{\mu_\rho^3}} (t-\tau) \sin(S_3) \sin\frac{j\pi v\tau}{\mu_L} d\tau\end{aligned} \tag{28}$$

4.2 Numerical characteristics of bridge response with road surface roughness

Similarly, from Eq. (20) and by using the RVFMM, the mean value of the bridge displacement considering the road surface roughnee can be expressed as :

$$\mu_{W(x,t)} = -\frac{2}{S_1\sqrt{\mu_\rho \mu_E \mu_I}} \sum_{j=1}^{\infty} \sin\frac{j\pi x}{\mu_L} \int_0^t ((\mu_{m_s}+\mu_{m_u})g - [\mu_{k_t}\mu_{r(x)} + \mu_{C_t}\mu_{\dot{r}(x)}]) \cdot S_2 \sin(S_3) \cdot \sin\frac{j\pi v\tau}{\mu_L} d\tau \tag{29}$$

The variance of bridge displacement can be computed by :

$$\begin{aligned}\sigma^2_{W(x,t)} = {} & [\frac{\partial W_{(x,t)}}{\partial m_s}]^2 \cdot \sigma^2_{m_s} + [\frac{\partial W(x,t)}{\partial m_u}]^2 \cdot \sigma^2_{m_u} + [\frac{\partial W_{(x,t)}}{\partial \rho}]^2 \cdot \sigma^2_{\rho} \\ & + [\frac{\partial W_{(x,t)}}{\partial L}]^2 \cdot \sigma^2_{L} + [\frac{\partial W_{(x,t)}}{\partial I}]^2 \cdot \sigma^2_{I} + [\frac{\partial W_{(x,t)}}{\partial E}]^2 \cdot \sigma^2_{E} + [\frac{\partial W_{(x,t)}}{\partial k_t}]^2 \cdot \sigma^2_{k_t} \\ & + [\frac{\partial W_{(x,t)}}{\partial C_t}]^2 \cdot \sigma^2_{C_t} + [\frac{\partial W_{(x,t)}}{\partial \varphi}]^2 \cdot \sigma^2_{\varphi}\end{aligned} \tag{30}$$

where

$$\frac{\partial W(x,t)}{\partial m_s} = -\frac{2((1+\mu_{m_u})g - [\mu_{k_t}\mu_{r(x)} + \mu_{C_t}\mu_{\dot{r}(x)}])}{S_1\sqrt{\mu_\rho \mu_E \mu_I}} \sum_{j=1}^{\infty} \sin\frac{j\pi \cdot x}{\mu_L} \cdot \int_0^t S_2 \sin(S_3) \sin\frac{j\pi v\tau}{\mu_L} d\tau \tag{31}$$

$$\frac{\partial W(x,t)}{\partial m_u} = -\frac{2((1+\mu_{m_s})g - [\mu_{k_t}\mu_{r(x)} + \mu_{C_t}\mu_{\dot{r}(x)}])}{S_1\sqrt{\mu_\rho \mu_E \mu_I}} \sum_{j=1}^{\infty} \sin\frac{j\pi \cdot x}{\mu_L} \cdot \int_0^t S_2 \sin(S_3) \sin\frac{j\pi v\tau}{\mu_L} d\tau \tag{32}$$

$$\begin{aligned}\frac{\partial W(x,t)}{\partial E} = {} & \frac{4(\mu_{m_u}+\mu_{m_s})g}{\mu_A \mu_\rho \mu_L \mu_{\omega_{dbj}}} \sum_{j=1}^{\infty} \sin\frac{j\pi \cdot x}{\mu_L} \\ & \int_0^t e^{-\mu_{\zeta_{bj}}\mu_{\omega_{bj}}(t-\tau)} \sin\mu_{\omega_{dbj}}(t-\tau) \sin\frac{j\pi v\tau}{\mu_L} d\tau + \frac{2}{\mu_A \mu_\rho \mu_L \mu_{\omega_{dbj}}} \cdot \\ & \int_0^t e^{-\mu_{\zeta_{bj}}\mu_{\omega_{bj}}(t-\tau)} \sin\mu_{\omega_{dbj}}(t-\tau) \cdot [\mu_{k_t}\mu_{r(x)} + \mu_{C_t}\mu_{\dot{r}(x)}] d\tau\end{aligned} \tag{33}$$

$$
\begin{aligned}
&\frac{\partial W(x,t)}{\partial I} \\
&= \frac{(\mu_{m_u}+\mu_{m_s})g}{S_1\sqrt{\mu_\rho \mu_E \mu_I^3}} \sum_{j=1}^{\infty} \sin\frac{j\pi\cdot x}{\mu_L} \int_0^t S_2 \sin(S_3) \sin\frac{j\pi v\tau}{\mu_L} d\tau \\
&+ \frac{2}{S_1\sqrt{\mu_\rho \mu_E \mu_I^3}} \cdot \int_0^t S_2 \sin(S_3) \cdot [\mu_{k_t}\mu_{r(x)} + \mu_{C_t}\mu_{\dot{r}(x)}] d\tau \\
&+ \frac{(\mu_{m_u}+\mu_{m_s})g}{S_1\sqrt{\mu_\rho \mu_E \mu_I}} \int_0^t S_2 \zeta_{bj} \frac{j^2\pi^2}{\mu_L^2} \cdot \sqrt{\frac{\mu_E}{\mu_I \mu_\rho}} (t-\tau) \sin(S_3) \sin\frac{j\pi v\tau}{\mu_L} d\tau \\
&+ \frac{2}{S_1\sqrt{\mu_\rho \mu_E \mu_I}} \cdot \int_0^t \frac{1}{2} \zeta_{bj} \frac{j^2\pi^2}{\mu_L^2} \cdot \sqrt{\frac{\mu_E}{\mu_I \mu_\rho}} (t-\tau) \sin(S_3) \cdot [\mu_{k_t}\mu_{r(x)} + \mu_{C_t}\mu_{\dot{r}(x)}] d\tau \\
&+ \frac{(\mu_{m_u}+\mu_{m_s})g}{S_1\sqrt{\mu_\rho \mu_E \mu_I}} \int_0^t S_2 \zeta_{bj} \frac{j^2\pi^2}{\mu_L^2} \cdot \sqrt{\frac{\mu_E}{\mu_I \mu_\rho}} (t-\tau) \cos(S_3) \sin\frac{j\pi v\tau}{\mu_L} d\tau \\
&+ \frac{2}{S_1\sqrt{\mu_\rho \mu_E \mu_I}} \cdot \int_0^t \frac{1}{2} \zeta_{bj} \frac{j^2\pi^2}{\mu_L^2} \cdot \sqrt{\frac{\mu_E}{\mu_I \mu_\rho}} (t-\tau) \cos(S_3) \cdot [\mu_{k_t}\mu_{r(x)} + \mu_{C_t}\mu_{\dot{r}(x)}] d\tau
\end{aligned}
\tag{34}
$$

$$
\begin{aligned}
&\frac{\partial W(x,t)}{\partial \rho} \\
&= \frac{(\mu_{m_u}+\mu_{m_s})g}{S_1\sqrt{\mu_\rho^3 \mu_E \mu_I}} \sum_{j=1}^{\infty} \sin\frac{j\pi\cdot x}{\mu_L} \int_0^t S_2 \sin(S_3) \sin\frac{j\pi v\tau}{\mu_L} d\tau \\
&+ \frac{2}{S_1\sqrt{\mu_\rho^3 \mu_E \mu_I}} \cdot \int_0^t S_2 \sin(S_3) \cdot [\mu_{k_t}\mu_{r(x)} + \mu_{C_t}\mu_{\dot{r}(x)}] d\tau \\
&+ \frac{(\mu_{m_u}+\mu_{m_s})g}{S_1\sqrt{\mu_\rho \mu_E \mu_I}} \int_0^t S_2 \zeta_{bj} \frac{j^2\pi^2}{\mu_L^2} \cdot \sqrt{\frac{\mu_E \mu_I}{\mu_\rho^3}} (t-\tau) \sin(S_3) \sin\frac{j\pi v\tau}{\mu_L} d\tau \\
&+ \frac{2}{S_1\sqrt{\mu_\rho \mu_E \mu_I}} \cdot \int_0^t \frac{1}{2} \zeta_{bj} \frac{j^2\pi^2}{\mu_L^2} \cdot \sqrt{\frac{\mu_E \mu_I}{\mu_\rho^3}} (t-\tau) \sin(S_3) \cdot [\mu_{k_t}\mu_{r(x)} + \mu_{C_t}\mu_{\dot{r}(x)}] d\tau \\
&+ \frac{(\mu_{m_u}+\mu_{m_s})g}{S_1\sqrt{\mu_\rho \mu_E \mu_I}} \int_0^t S_2 \zeta_{bj} \frac{j^2\pi^2}{\mu_L^2} \cdot \sqrt{\frac{\mu_E \mu_I}{\mu_\rho^3}} (t-\tau) \cos(S_3) \sin\frac{j\pi v\tau}{\mu_L} d\tau \\
&+ \frac{2}{S_1\sqrt{\mu_\rho \mu_E \mu_I}} \cdot \int_0^t \frac{1}{2} \zeta_{bj} \frac{j^2\pi^2}{\mu_L^2} \cdot \sqrt{\frac{\mu_E \mu_I}{\mu_\rho^3}} (t-\tau) \cos(S_3) \cdot [\mu_{k_t}\mu_{r(x)} + \mu_{C_t}\mu_{\dot{r}(x)}] d\tau
\end{aligned}
\tag{35}
$$

$$
\begin{aligned}
&\frac{\partial W(x,t)}{\partial L} \\
&= \frac{(\mu_{m_u}+\mu_{m_s})g}{S_1\sqrt{\mu_\rho^3\mu_E\mu_I}}\sum_{j=1}^{\infty}\sin\frac{j\pi\cdot x}{\mu_L}\int_0^t S_2\sin(S_3)\sin\frac{j\pi v\tau}{\mu_L}d\tau \\
&+ \frac{2}{S_1\sqrt{\mu_\rho^3\mu_E\mu_I}}\cdot\int_0^t S_2\sin(S_3)\cdot[\mu_{k_t}\mu_{r(x)}+\mu_{C_t}\mu_{\dot r(x)}]d\tau \\
&+ \frac{(\mu_{m_u}+\mu_{m_s})g}{S_1\sqrt{\mu_\rho\mu_E\mu_I}}\int_0^t S_2\zeta_{bj}\frac{j^2\pi^2}{\mu_L^2}\cdot\sqrt{\frac{\mu_E\mu_I}{\mu_\rho^3}}(t-\tau)\sin(S_3)\sin\frac{j\pi v\tau}{\mu_L}d\tau \\
&+ \frac{2}{S_1\sqrt{\mu_\rho\mu_E\mu_I}}\cdot\int_0^t \frac{1}{2}\zeta_{bj}\frac{j^2\pi^2}{\mu_L^2}\cdot\sqrt{\frac{\mu_E\mu_I}{\mu_\rho^3}}(t-\tau)\sin(S_3)\cdot[\mu_{k_t}\mu_{r(x)}+\mu_{C_t}\mu_{\dot r(x)}]d\tau \\
&+ \frac{(\mu_{m_u}+\mu_{m_s})g}{S_1\sqrt{\mu_\rho\mu_E\mu_I}}\int_0^t S_2\zeta_{bj}\frac{j^2\pi^2}{\mu_L^2}\cdot\sqrt{\frac{\mu_E\mu_I}{\mu_\rho^3}}(t-\tau)\cos(S_3)\sin\frac{j\pi v\tau}{\mu_L}d\tau \\
&+ \frac{2}{S_1\sqrt{\mu_\rho\mu_E\mu_I}}\cdot\int_0^t \frac{1}{2}\zeta_{bj}\frac{j^2\pi^2}{\mu_L^2}\cdot\sqrt{\frac{\mu_E\mu_I}{\mu_\rho^3}}(t-\tau)\cos(S_3)\cdot[\mu_{k_t}\mu_{r(x)}+\mu_{C_t}\mu_{\dot r(x)}]d\tau
\end{aligned}
\tag{36}
$$

$$
\begin{aligned}
\frac{\partial W(x,t)}{\partial k_t} &= -\frac{2((\mu_{m_s}+\mu_{m_u})g-[\mu_{r(x)}+\mu_{C_t}\mu_{\dot r(x)}])}{S_1\sqrt{\mu_\rho\mu_E\mu_I}}\sum_{j=1}^{\infty}\sin\frac{j\pi\cdot x}{\mu_L} \\
&\cdot\int_0^t S_2\sin(S_3)\sin\frac{j\pi v\tau}{\mu_L}d\tau
\end{aligned}
\tag{37}
$$

$$
\begin{aligned}
\frac{\partial W(x,t)}{\partial C_t} &= -\frac{2((\mu_{m_s}+\mu_{m_u})g-[\mu_{k_t}\mu_{r(x)}+\mu_{\dot r(x)}])}{S_1\sqrt{\mu_\rho\mu_E\mu_I}}\sum_{j=1}^{\infty}\sin\frac{j\pi\cdot x}{\mu_L} \\
&\cdot\int_0^t S_2\sin(S_3)\sin\frac{j\pi v\tau}{\mu_L}d\tau
\end{aligned}
\tag{38}
$$

$$
\begin{aligned}
\frac{\partial W(x,t)}{\partial \varphi} &= -\frac{2((\mu_{m_s}+\mu_{m_u})g-[\mu_{k_t}\mu_{\dot r(x)}+\mu_{C_t}\mu_{r(x)}])}{S_1\sqrt{\mu_\rho\mu_E\mu_I}}\sum_{j=1}^{\infty}\sin\frac{j\pi\cdot x}{\mu_L} \\
&\cdot\int_0^t S_2\sin(S_3)\sin\frac{j\pi v\tau}{\mu_L}d\tau
\end{aligned}
\tag{39}
$$

5 Numerical Simulations

Vehicle's and bridge's parameters are considered as random variables in the following examples. The mean value of system parameters used in the numerical simulations are given in Tables 1 and 2. The vehicle is typical for a lightly damped passenger car [Türkay and Akçay (2005)].

Table 1: Parameters of the bridge model

Description	Notation	Value
Length of the bridge	L	$40m$
Moment of inertia	I	$0.15m^4$
Damping ratio	ζ	0.05
Young's modulus	E	$3.2\times10^{10}N/m^2$
Mass density	ρ	$5200kg/m^3$

Table 2: Parameters of the vehicle model

Description	Notation	Value
Sprung mass	m_s	$1600kg$
Unsprung mass	m_u	$160kg$
Suspension damping	C_s	$960Ns/m$
Tire damping	C_t	$960Ns/m$
Suspension stiffness	K_s	$1.8\times10^7N/m$
Vehicle stiffness	K_t	$7.2\times10^7N/m$

5.1 Random response analysis of vehicle-bridge system with smooth road surface

Two different vehicle's speed, $v=5m/s$ and $v=20m/s$, are used to investigate the influence caused by vehicle's speed on bridge response. The corresponding bridge displacement responses at mid-span are shown in Figures 2 and 3, respectively. The amplitude of the bridge mid-span displacement in Figure 3 is bigger than that in Figure 2, which means the bridge displacement response increases along with the increase of the vehicle speed. Meanwhile, the period of periodic displacement response of the bridge is longer for lower moving speed of the vehicle. It can also be observed from Figures 2 and 3 that the maximum amplitudes of bridge response at its mid-span do not occur at the time when the vehicle pass this position. The similar phenomenon can also be found in research literature [Yang and Lin (2005)].

The bridge's Young's modulus, mass density and moment of inertia as well as vehicle's sprung and unsprung masses are considered as random variables. Their mean values are shown in Tables 1 and 2. To investigate the effects of system parameters on the bridge response, the randomness of each of parameters is considered separately first and then simultaneously. The coefficient of variation (COV, that is the ratio of the standard deviation to mean value of a random variable)is assumed as 0.05 for random variables m_s, m_u, ρ, E, I. The velocity of vehicle is constant ($v = 5m/s$). The standard deviations (SD) of the bridge mid-span displacement response are given in Figures 4(a)-(f)to demonstrate the changes of bridge responses produced by the uncertainty of system parameters. From Figures 4(a)and 4(b), it can be seen that the vehicle's sprung and unsprung masses produce the similar effects on the bridge response. The elastic modulus and inertia moment of area of the bridge have quite similar influences on the bridge response, and the changes of the bridge response caused by their uncertainties are bigger than that caused by the mass per unit, which can be found from Figures 4(c)-(e). Comparing Figures 4(a)-(b) with 4(c)-(e), it can be observed that the standard deviations of bridge response caused by the randomness of its own parameters are greater than those caused by vehicle' parameters. In other words, vehicle response is more sensitive to the uncertainty of bridge parameters. Figure 4(f) shows that the standard deviation of bridge response becomes significant big if the randomness of all parameters is considered simultaneously.

In order to validate the method presented in this paper, Monte Carlo simulation method is used as a reference approach. The standard deviations obtained by 10000 Monte Carlo simulations are also shown in Figures 4(a)-(f). In addition, the mean value and standard deviation of bridge mid-span response calculated by the proposed method and Monte Carlo simulations are given in Figures 5 and 6, respectively, when the coefficient of variation of all random parameters is taken as 0.1. The relative errors between the results obtained by the two methods and the consumed time are listed in Tables 3-9.

In general, computational results obtained by the proposed method (RVFMM) are in good agreement with those computed by the Monte-Carlo simulation method. The results obtained by the two methods agree with very well when the coefficient of variation of random system parameters is small as shown in Figure 4 and Tables 3-8. The relative error is increased when the variations of random parameters become bigger as shown in Figure 5 and Table 9. In Table 9, the relative error is still acceptable when the vehicle's and bridge's parameters are considered as random variables simultaneously and their coefficients of variation are equals to 0.1. The accuracy of the RVFMM can be improved if the second-order Taylor expansion is used. It can be expected that the relative errors will be smaller if more simulations

are also used in the Monte Carlo method. From Tables 3-9, it can be also found that the time consumed by the Monte Carlo simulation is much greater than that used by the proposed method.

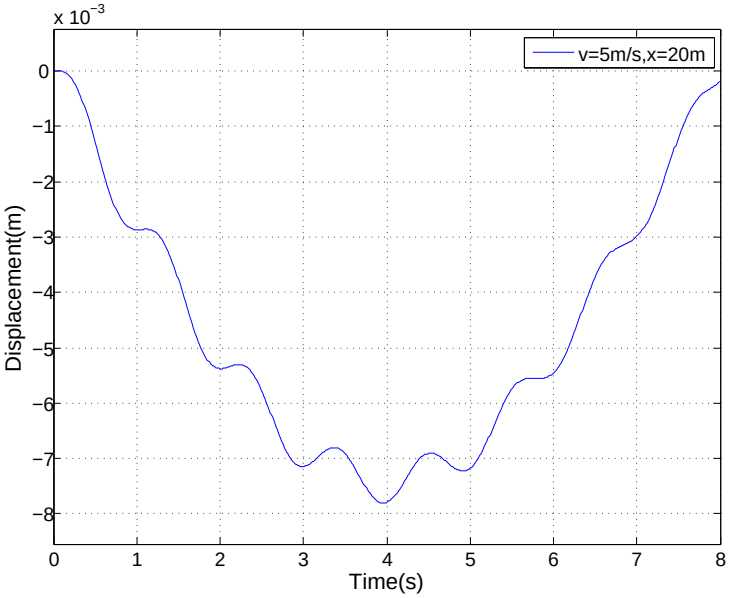

Figure 2: Displacement response of bridge mid-span $(v = 5m/s, x = 20m)$.

Table 3: Comparison of results obtained from two different methods

Time(s)		1.6	2.8	3.6	4.4	time
$COV(m_1) = 0.05$	RVFMM	1.12E-05	1.71E-05	1.86E-05	1.79E-05	6.25s
	MCSM	1.13E-05	1.71E-05	1.86E-05	1.79E-05	7.53hrs
	Relative error	0.17%	0.18%	0.22%	0.15%	

Table 4: Comparison of results obtained from two different methods

Time(s)		1.6	2.8	3.6	4.4	time
$COV(m_2) = 0.05$	RVFMM	1.72e-04	1.07e-04	2.54e-04	2.81e-04	6.38s
	MCSM	1.72e-05	1.07e-05	2.55e-05	2.82e-05	7.86hrs
	Relative error	0.09%	0.08%	0.39%	0.35%	

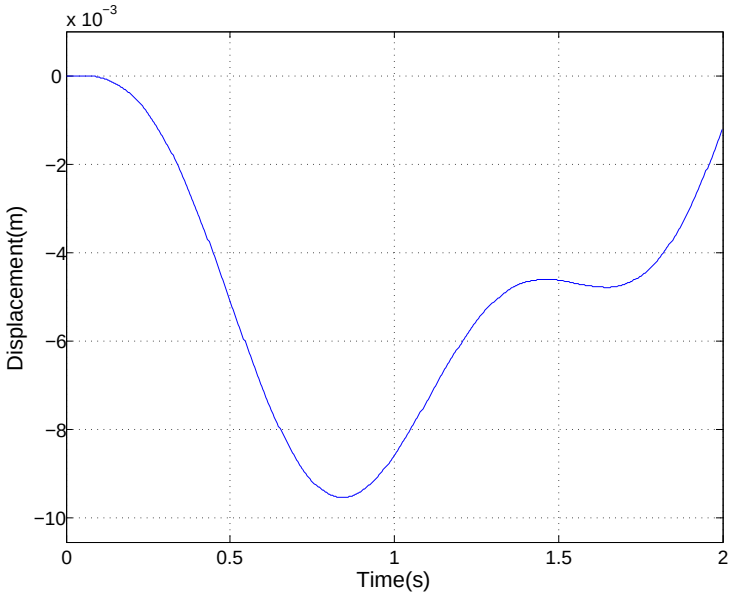

Figure 3: Displacement response of bridge mid-span $(v = 20m/s, x = 20m)$.

Table 5: Comparison of results obtained from two different methods

Time(s)		1.6	2.8	3.6	4.4	time
$COV(E) = 0.05$	RVFMM	4.96e-05	1.12e-03	1.15e-03	6.62e-04	5.486s
	MCSM	4.95e-04	1.11e-03	1.15e-03	6.64e-04	6.29hrs
	Relative error	0.20%	0.90%	0.09%	0.30%	

Table 6: Comparison of results obtained from two different methods

Time(s)		1.6	2.8	3.6	4.4	time
$COV(\rho) = 0.05$	RVFMM	3.33e-04	9.15e-04	9.98e-04	7.33e-04	4.256s
	MCSM	3.33e-04	9.12e-04	9.98e-04	7.35e-04	5.29hrs
	Relative error	0.06%	0.33%	0.07%	0.27%	

Table 7: Comparison of results obtained from two different methods

Time(s)		1.6	2.8	3.6	4.4	time
$COV(I) = 0.05$	RVFMM	4.96e-05	1.11e-03	1.16e-03	6.62e-04	4.569s
	MCSM	4.96e-04	1.11e-03	1.15e-03	6.63e-04	5.97hrs
	Relative error	0.09%	0.13%	0.86%	0.15%	

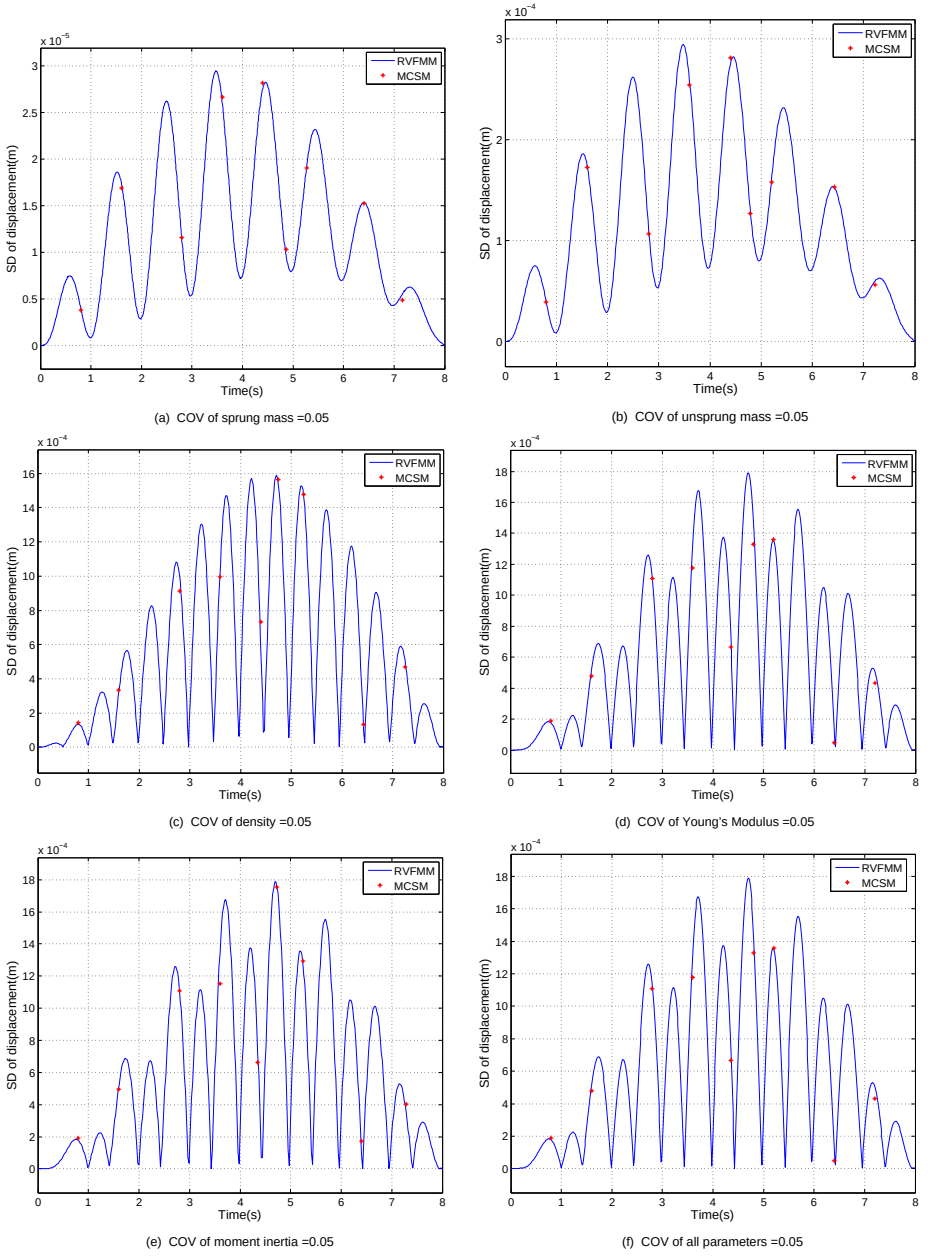

Figure 4: Standard deviation of bridge mid-span displacement.

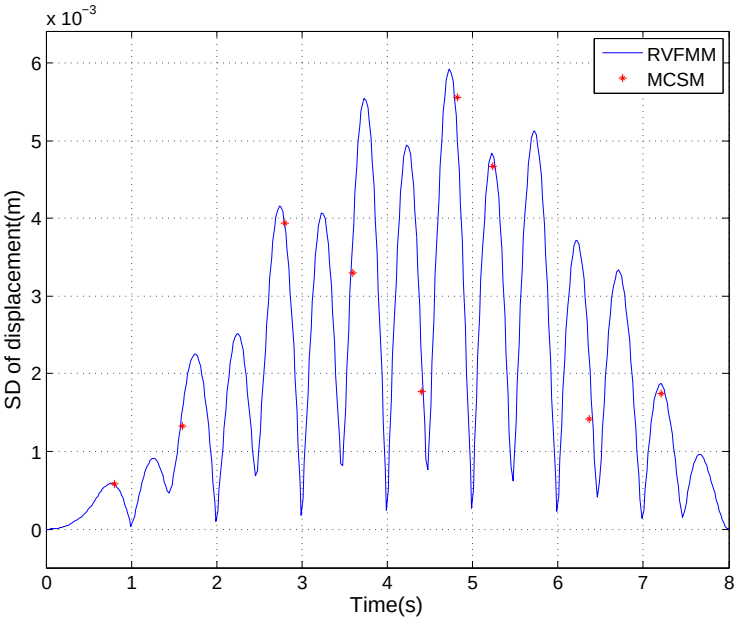

Figure 5: Standard deviation of bridge mid-span displacement (COV of all parameters is 0.1).

Table 8: Comparison of results obtained from two different methods

Time(s)		1.6	2.8	3.6	4.4	time
$COV(all) = 0.05$	RVFMM	7.70e-04	1.81e-03	2.15e-03	1.32e-03	12.138s
	MCSM	7.66e-04	1.81e-03	2.16e-03	1.32e-03	10.58hrs
	Relative error	0.52%	0.08%	0.46%	0.12%	

Table 9: Comparison of results obtained from two different methods

Time(s)		1.6	2.8	3.6	4.4	time
$COV(all) = 0.1$	RVFMM	1.35e-03	3.96e-03	3.33e-03	1.79e-03	13.486s
	MCSM	1.33e-03	3.94e-03	3.30e-03	1.77e-03	11.29hrs
	Relative error	1.35%	0.53%	1.06%	1.18%	

5.2 Random response analysis of vehicle-bridge system with road surface roughness

The road surface roughness of bridge can significantly change the force exerted on the bridge by the moving vehicle. According to ISO8068 and Honda et al [Honda,

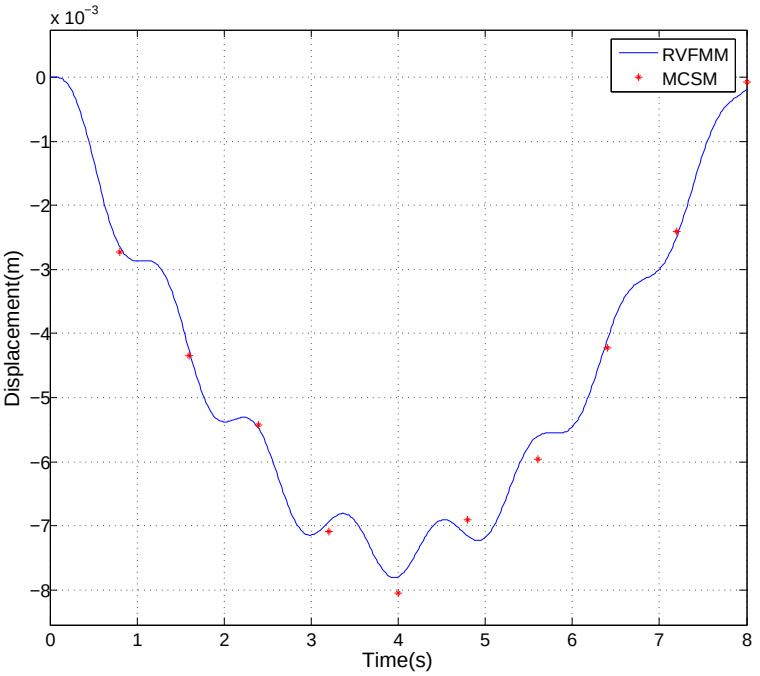

Figure 6: Mean value of bridge mid-span displacement (COV of all parameters is 0.1).

Kajikawa, and Kobori (1982)], the road surface is considered as a random process with a Gaussian probability distribution and the road roughness coefficient is assuming as $2 \times 10^{-6} m^2/rad/m$. The interactive force caused by the road roughness and the moving vehicle is shown in Figure 7 when the velocity of vehicle is $5m/s$. It should be noted that this force is a random process but the effects of the randomness of vehicle's and bridge's parameters are not included.

The bridge's Young's modulus, mass density and moment of inertia as well as vehicle's sprung mass, unsprung masses, tire stiffness and damping are considered as random variables in this part.The mean value and standard deviation of the displacement response of the bridge mid-span for smooth and rough road conditions are shown in Figures 8 and 9, respectively. It can be easily observed that the bridge response is greatly increased when the road surface roughness is considered as shown in Figure 8. The standard deviation of the rough road condition is also bigger than that of the smooth road condition in Figure 9 as expected.

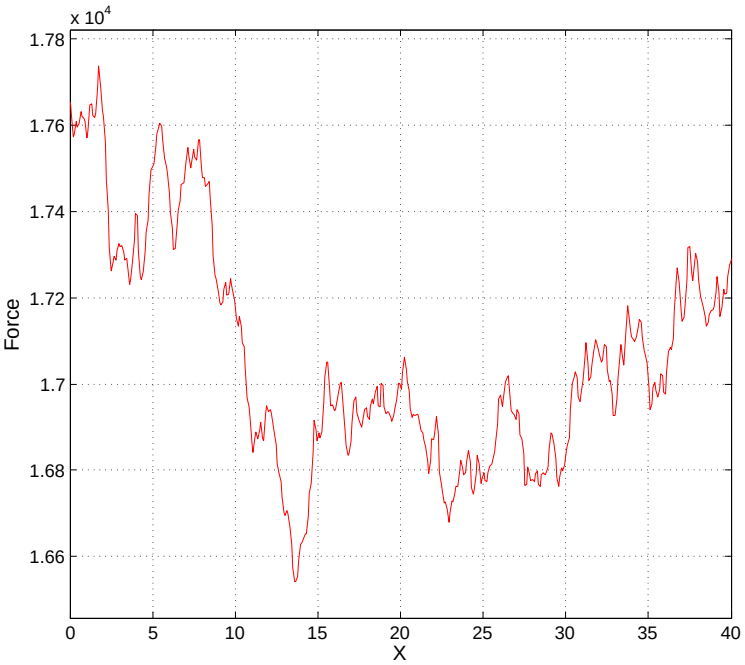

Figure 7: Interactive force with road surface roughness.

6 Conclusions

The dynamic response of bridge under moving vehicle is investigated in this paper. The uncertainties in the vehicle-bridge interaction system are considered and vehicle's and bridge's parameters are modeled as random variables. Two different road conditions, smooth road surface and rough road surface, are also included in the model for the dynamic analysis of the vehicle-bridge coupled system. The modal superposition method and random variable's functional moment method (RVFMM) are employed to predict the first and second moments of the bridge response. The effects produced by the individual system parameters and road roughness on the bridge response are demonstrated by numerical examples. The effectiveness of the presented method are validated by the Monte Carlo simulation method.

The accuracy of the presented method can be improved if the second-order Taylor expansion is adopted in the RVFMM but it requires more computational effort. The method can be further developed for dynamic analysis of vehicle-bridge interaction system using complex models such as bridge and full car,bridge and multi vehicle as well as vehicle and multi-span bridge models. The RVFMM could be combined

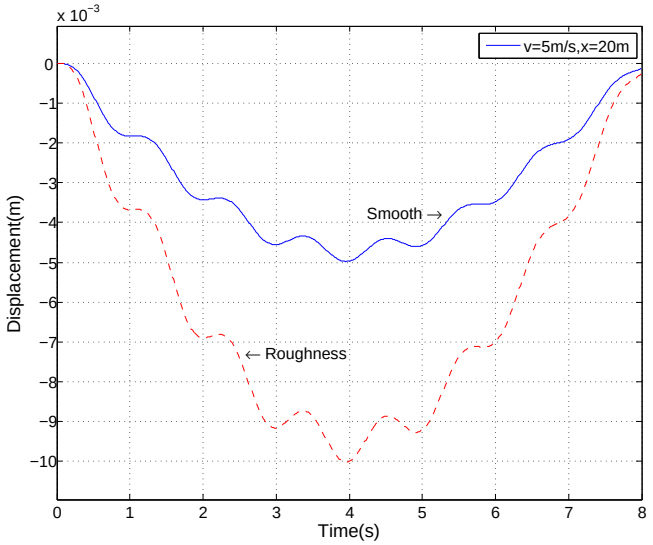

Figure 8: Mean value of bridge mid-span displacement with different road conditions.

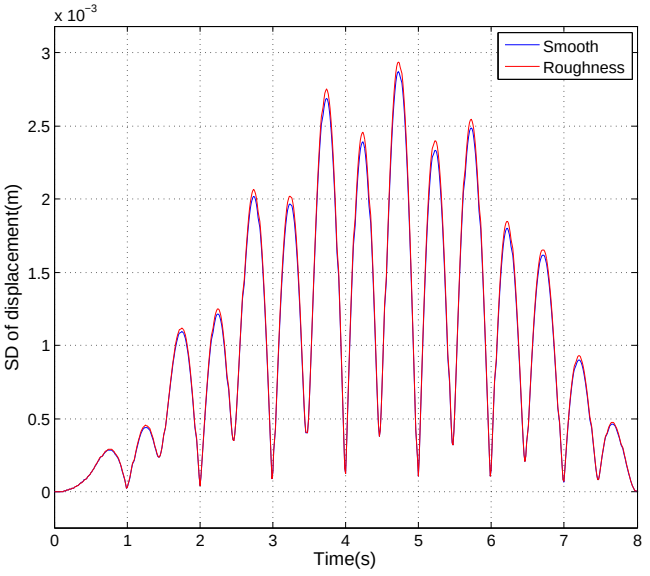

Figure 9: Standard deviation of bridge mid-span displacement with different road conditions.

with other methods rather than superposition method for the dynamic analysis of train-bridge system if it is modeled as a time-dependent system.

Acknowledgement: The work reported in this paper was supported by the Australian Research Council through ARC Discovery Grants.

References

Au, F.; Cheng, Y.; Cheung, Y. (2001): Effects of random road surface roughness and long-term deflection of prestressed concrete girder and cable-stayed bridges on impact due to moving vehicles. *Computers & Structures*, vol. 79, no. 8, pp. 853–872.

Baroth, J.; Bressolette, P.; Chauvière, C.; Fogli, M. (2007): An efficient SFE method using Lagrange polynomials: Application to nonlinear mechanical problems with uncertain parameters. *Computer methods in applied mechanics and engineering*, vol. 196, no. 45-48, pp. 4419–4429.

Dey, S. S.; Balasubramanian, N. (1984): Dynamic response of orthotropic curved bridge decks due to moving loads. *Computers and Structures*, vol. 18, no. 1, pp. 27 – 32.

Ding, L.; Hao, H.; Zhu, X. (2009): Evaluation of dynamic vehicle axle loads on bridges with different surface conditions. *Journal of Sound and Vibration*, vol. 323, no. 3-5, pp. 826–848.

Fryba, L. (1999): Vibration of solids and structures under moving loads. *Telford, London*.

Gaignaire, R.; Clénet, S.; Sudret, B.; Moreau, O. (2007): 3-D spectral stochastic finite element method in electromagnetism. *Magnetics, IEEE Transactions on*, vol. 43, no. 4, pp. 1209–1212.

Gao, W. (2007): Random seismic response analysis of truss structures with uncertain parameters. *Engineering Structures*, vol. 29, no. 7, pp. 1487–1498.

Gao, W.; Song, C.; Tin-Loi, F. (2009): Probabilistic Interval Response and Reliability Analysis of Structures with A Mixture of Random and Interval Properties. *CMES: Computer Modeling in Engineering & Sciences*, vol. 46, no. 2, pp. 151–190.

Gao, W.; Song, C.; Tin-Loi, F. (2010): Probabilistic interval analysis for structures with uncertainty. *Structural Safety*, vol. 32, no. 3, pp. 191–199.

Gao, W.; Zhang, N.; Dai, J. (2008): A stochastic quarter-car model for dynamic analysis of vehicles with uncertain parameters. *Vehicle System Dynamics*, vol. 46, no. 12, pp. 1159–1169.

Ghanem, R.; Spanos, P. (2003): *Stochastic finite elements: a spectral approach*. Dover Pubns.

Green, M.; Cebon, D. (1994): Dynamic response of highway bridges to heavy vehicle loads: theory and experimental validation. *Journal of Sound and Vibration*, vol. 170, no. 1, pp. 51–78.

Gupta, A.; Hughes, K.; Sellars, C. (1980): Glass-Lubricated Hot Extrusion of Stainless Steel. *Met. Technol.*, vol. 7, no. 8, pp. 323–331.

Honda, H.; Kajikawa, Y.; Kobori, T. (1982): Spectra of road surface roughness on bridges. *Journal of the Structural Division*, vol. 108, no. 9, pp. 1956–1966.

Hwang, E.; Nowak, A. (1991): Simulation of dynamic load for bridges. *Journal of Structural Engineering*, vol. 117, pp. 1413.

Kim, C.; Kawatani, M.; Kim, K. (2005): Three-dimensional dynamic analysis for bridge-vehicle interaction with roadway roughness. *Computers & Structures*, vol. 83, no. 19-20, pp. 1627–1645.

Kwasniewski, L.; Li, H.; Wekezer, J.; Malachowski, J. (2006): Finite element analysis of vehicle-bridge interaction. *Finite Elements in Analysis and Design*, vol. 42, no. 11, pp. 950–959.

Law, S.; Zhu, X. (2005): Bridge dynamic responses due to road surface roughness and braking of vehicle. *Journal of Sound and Vibration*, vol. 282, no. 3-5, pp. 805–830.

Manjuprasad, M.; Manohar, C. (2007): Adaptive random field mesh refinements in stochastic finite element reliability analysis of structures. *CMES: Computer Modeling in Engineering & Sciences*, vol. 19, no. 1, pp. 23.

Marek, P.; Brozzetti, J.; Gustar, M.; Elishakoff, I. (2002): Probabilistic Assessment of Structures using Monte Carlo Simulations. *Applied Mechanics Reviews*, vol. 55, pp. B31.

Muscolino, G.; Ricciardi, G.; Impollonia, N. (2000): Improved dynamic analysis of structures with mechanical uncertainties under deterministic input. *Probabilistic Engineering Mechanics*, vol. 15, no. 2, pp. 199–212.

Radhika, B.; Panda, S.; Manohar, C. (2008): Time Variant Reliability Analysis of Nonlinear Structural Dynamical Systems using combined Monte Carlo Simulations and Asymptotic Extreme Value Theory. *CMES: Computer Modeling in Engineering & Sciences*.

Rassem, M.; Ghobarah, A.; Heidebrecht, A. (1996): Site effects on the seismic response of a suspension bridge. *Engineering Structures*, vol. 18, no. 5, pp. 363–370.

Sridharan, N.; Mallik, A. (1979): Numerical analysis of vibration of beams subjected to moving loads. *Journal of Sound Vibration*, vol. 65, pp. 147–150.

Türkay, S.; Akçay, H. (2005): A study of random vibration characteristics of the quarter-car model. *Journal of Sound and Vibration*, vol. 282, no. 1-2, pp. 111–124.

Wu, J.; Dai, C. (1987): Dynamic responses of multispan nonuniform beam due to moving loads. *Journal of Structural Engineering*, vol. 113, pp. 458.

Wu, S.; Law, S. (2010): Dynamic analysis of bridge-vehicle system with uncertainties based on finite element model. *Probabilistic Engineering Mechanics*.

Wu, S.; Law, S. (2010): Moving force identification based on stochastic finite element model. *Engineering Structures*, vol. 32, no. 4, pp. 1016–1027.

Xia, Y.; Hao, H.; Brownjohn, J.; Xia, P. (2002): Damage identification of structures with uncertain frequency and mode shape data. *Earthquake Engineering & Structural Dynamics*, vol. 31, no. 5, pp. 1053–1066.

Yang, Y.; Chang, K. (2009): Extracting the bridge frequencies indirectly from a passing vehicle: Parametric study. *Engineering Structures*, vol. 31, no. 10, pp. 2448–2459.

Yang, Y.; Chang, K. (2009): Extraction of bridge frequencies from the dynamic response of a passing vehicle enhanced by the EMD technique. *Journal of sound and vibration*, vol. 322, no. 4-5, pp. 718–739.

Yang, Y.; Lin, C. (2005): Vehicle-bridge interaction dynamics and potential applications. *Journal of sound and vibration*, vol. 284, no. 1-2, pp. 205–226.

Yang, Y.; Wu, Y. (2001): A versatile element for analyzing vehicle-bridge interaction response. *Engineering Structures*, vol. 23, no. 5, pp. 452–469.

Yin, X.; Fang, Z.; Cai, C.; Deng, L. (2010): Non-stationary random vibration of bridges under vehicles with variable speed. *Engineering Structures*.